Journal of Organometallic Chemistry 696 (2011) 321–330

Contents lists available at ScienceDirect

Journal of Organometallic Chemistry

journal homepage: www.elsevier.com/locate/jorganchem

Linked bis(β-diketiminato) yttrium and lanthanum complexes as catalysts in asymmetric hydroamination/cyclization of aminoalkenes (AHA)

Daniela V. Vitanova [a], Frank Hampel [a], Kai C. Hultzsch [b,*]

[a] Institut für Organische Chemie, Friedrich-Alexander Universität Erlangen-Nürnberg, Henkestr. 42, D-91054 Erlangen, Germany
[b] Department of Chemistry and Chemical Biology, Rutgers, The State University of New Jersey, 610 Taylor Road, Piscataway, NJ 08854-8087, USA

ARTICLE INFO

Article history:
Received 1 August 2010
Received in revised form
21 September 2010
Accepted 22 September 2010
Available online 1 October 2010

Keywords:
Asymmetric catalysis
Hydroamination
Rare-earth metals
β-Diketiminato complexes

ABSTRACT

Linked bis(β-diketiminato) rare-earth metal complexes based on the ethylene-bridged ligand $[C_2H_4(BDI^{DClP})_2]H_2$ [DClP = 2,6-$Cl_2C_6H_3$] and the cyclohexyl-bridged ligands $[Cy(BDI^{Ar})_2]H_2$ [Ar = PMP (= *p*-$MeOC_6H_4$), Mes (= 2,4,6-$Me_3C_6H_2$), DIPP (= 2,6-*i*$Pr_2C_6H_3$)] were prepared via amine elimination starting from $[Ln\{N(SiMe_3)_2\}_3]$ (Ln = La, Y). The three cyclohexyl-bridged complexes [{(*R*,*R*)-$Cy(BDI^{Mes})_2$}$YN(SiMe_3)_2$] ((*R*,*R*)-**3**), [{(*R*,*R*)-$Cy(BDI^{Mes})_2$}$LaN(SiMe_3)_2$] ((*R*,*R*)-**4**), and [{(*R*,*R*)-$Cy(BDI^{DIPP})_2$}$LaN(SiMe_3)_2$] ((*R*,*R*)-**5**) were obtained enantiomerically pure. The X-ray crystal structure analysis of the racemic variants of **3** and **4** revealed a distorted square pyramidal coordination geometry around the rare-earth metal, in which the amido ligand occupies the apical position and the two linked β-diketiminato moieties form the basis. The two aromatic substituents adopt a *transoid* arrangement and both β-diketiminato moieties are bound in a η^5 coordination mode with close Ln···C contacts. Due to the smaller ionic radius of yttrium vs. lanthanum, the front side of the yttrium complex **3** is sterically more hindered than in the lanthanum complex **4**, but there is much more empty coordination space on the rear side, which may rationalize the observed differences in selectivity of **3** in comparison to **4**. The catalytic efficiency of the β-diketiminato complexes was strongly affected by steric factors such as ionic radius of the metal and the steric bulk of the aryl substituents, which is an indication for highly steric encumbered catalytic species. The complexes displayed good to moderate catalytic activity in the hydroamination/cyclization of aminoalkenes depending on the steric hindrance around the metal center. The sterically most demanding diisopropylphenyl-substituted complex (*R*,*R*)-**5** displayed significantly higher enantioselectivities (up to 76% ee), but lower catalytic activity in comparison to the sterically more open mesityl-substituted complex (*R*,*R*)-**4**. The smaller yttrium metal center in complex (*R*,*R*)-**3** led to reduced activity as well as a reversal in enantioselectivity, which may be rationalized by a change of the approach of the alkene moiety to the Ln-amido bond in the cyclization transition state.

© 2010 Elsevier B.V. All rights reserved.

1. Introduction

The hydroamination is a highly atom economical process in which an amine N–H bond is added to an unsaturated carbon–carbon bond. This reaction is of great potential interest for the waste-free synthesis of basic and fine chemicals, pharmaceuticals and other industrially relevant building blocks starting from inexpensive precursors [1,2].

Intensive research efforts from a growing number of research group has led to the development of a variety of catalytic systems based on alkali or alkaline-earth metals [2a,3], early (group 3–5, as well as lanthanides and actinides) [2c–f,h,j,l] and late (group 8–10) [2b,g,i,k] transition metals. Rare-earth metal-based catalysts [4], pioneered by Marks and co-workers [2f,5], are still among the most reactive and versatile systems.

The generation of new stereogenic centers during the hydroamination process is an attractive application of this reaction and the asymmetric hydroamination has found increased interest in recent years [6], in particular for catalyst systems facilitating the enantioselective cyclization of aminoalkenes [5b–e,7–9]. Most of these chiral catalyst systems have C_2-symmetry, while the number of catalysts with C_1-symmetry is rather limited [5b,e,8e,9e].

We have previously investigated various C_1 symmetric linked bis(β-diketiminato) rare-earth metal complexes [10–12] as catalysts in the epoxide/CO_2-copolymerization and the catalytic activity of related group IV metal complexes in ethylene polymerization was recently reported [13,14]. Herein we want to disclose the catalytic activity of these linked bis(β-diketiminato) rare-earth

* Corresponding author. Fax: +1 732 445 5312.
E-mail address: hultzsch@rci.rutgers.edu (K.C. Hultzsch).

0022-328X/$ – see front matter © 2010 Elsevier B.V. All rights reserved.
doi:10.1016/j.jorganchem.2010.09.051

metal complexes in hydroamination/cyclization reactions and their effectiveness to perform enantioselective reactions.

2. Results and discussion

2.1. Synthesis of linked bis(β-diketiminato) lanthanum and yttrium complexes

2.1.1. Synthesis of linked bis(β-diketiminato) ligands

As reported previously [10], various linked bis(β-diketiminato) ligands can be prepared through a two-step standard condensation route (Scheme 1). Reaction of 2,4-pentadione and an aniline derivative yields a β-enaminoketone. The carbonyl function of this intermediate was activated using Meerwein's salt, $[Et_3O]^+[BF_4]^-$, in order to introduce the ethylenediamine or *trans*-cyclohexane-1,2-diamine linkers. Thus, utilization of resolved *trans*-(*R*,*R*)-1,2-diaminocyclohexane provides access to the enantiomerically pure ligands [(*R*,*R*)-Cy(BDI^{Mes})$_2$]H$_2$ and [(*R*,*R*)-Cy(BDI^{DIPP})$_2$]H$_2$. The two new ligands [C$_2$H$_4$(BDI^{DClP})$_2$]H$_2$ (DClP = 2,6-Cl$_2$C$_6$H$_3$) and [Cy(BDI^{PMP})$_2$)$_2$]H$_2$ (PMP = *p*-MeOC$_6$H$_4$) were prepared to probe the electronic influence of the aromatic substituent on catalytic activity.

2.1.2. Complex synthesis and structural characterization

The rare-earth metal complexes are most conveniently prepared via amine elimination starting from the homoleptic trisamide [Ln{N(SiMe$_3$)$_2$}$_3$] (Ln = La, Y). While the reaction of the sterically less hindered trisamide [Ln{N(SiHMe$_2$)$_2$}$_3$(THF)$_2$] proceed generally under milder reaction conditions [10b], the resulting bis(dimethylsilyl)amido complexes were considered less suitable for catalytic hydroamination. Previous studies [7b,15] have shown that bis(dimethylsilyl)amido complexes require higher reaction temperatures and only a fraction of the complex is catalytically active during the reaction. This hampered catalyst activation is a result of the lower basicity of the bis(dimethylsilyl)amido ligand (pK_a [HN(SiHMe$_2$)$_2$] = 22.8 [16a]) compared to the bis(trimethylsilyl)amido ligand (pK_a [HN(SiMe$_3$)$_2$] = 25.8 [16b]).

The reaction of the 2,6-dichlorophenyl-substituted ethylene-linked bis(β-diketiminato) ligand [C$_2$H$_4$(BDI^{DClP})$_2$]H$_2$ with [La{N(SiMe$_3$)$_2$}$_3$] proceeded cleanly at 65 °C in toluene within 3 h to produce **1** in high yield (Scheme 2). In agreement to previously characterized ethylene-linked bis(β-diketiminato) rare-earth metal complexes [10], the ^{1}H and ^{13}C NMR spectra of complex **1** are in accordance with a C_s symmetric structure in solution on the NMR time scale. The SiCH$_3$ groups and the methine proton of the β-diketiminato ligand each give rise to one signal and the ethylene protons are split into two AA′BB′ doublets of triplets in the ^{1}H NMR spectrum.

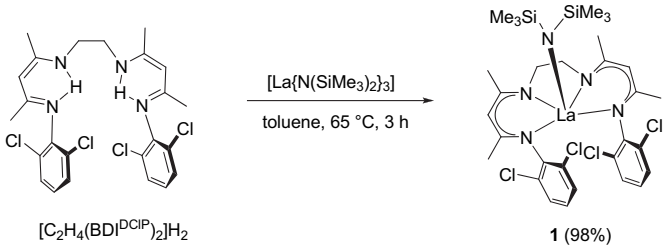

Scheme 2.

As noted previously [10], the reactions of the more rigid cyclohexyl-bridged ligands require commonly harsher reaction conditions than the corresponding ethylene-bridged ligands. The reaction conditions also depend significantly on the steric demand of the aromatic substituent and the size of the rare-earth metal. The reaction of the sterically least hindered *p*-methoxyphenyl-substituted racemic ligand [Cy(BDI^{PMP})$_2$]H$_2$ with [La{N(SiMe$_3$)$_2$}$_3$] proceeded readily in refluxing hexanes within 2 h to form *rac*-**2** in 68% yield (Scheme 3). The sterically more congested mesityl- and 2,6-diisopropylphenyl-substituted ligands required increasingly higher reaction temperatures to form the corresponding lanthanum complexes. The enantiopure complexes (*R*,*R*)-**4** (toluene, 100 °C, 6 h) and (*R*,*R*)-**5** (toluene, 110 °C, 9 d) were prepared using slightly higher reaction temperatures in comparison to the synthesis of their racemic counterparts [10] in order to improve the yield. The smaller yttrium was less reactive than lanthanum and the reaction of [(*R*,*R*)-Cy(BDI^{Mes})$_2$]-H$_2$ with [Y{N(SiMe$_3$)$_2$}$_3$] required significant harsher reaction conditions and longer reaction times to generate (*R*,*R*)-**3** (toluene, 120 °C, 8 d). The complexation of yttrium was also aided by the addition of two equiv of THF, although the product was isolated as a THF-free complex.

The ^{1}H and ^{13}C NMR spectra of the cyclohexyl-bridged complexes (*R*,*R*)-**4** and (*R*,*R*)-**5** are identical to their racemic counterparts [10]. The spectra of the yttrium complex (*R*,*R*)-**3** are in accordance with a C_1 symmetric structure in solution at room temperature based on the observation of two different β-diketiminato groups and two diastereotopic aromatic rings. However, the

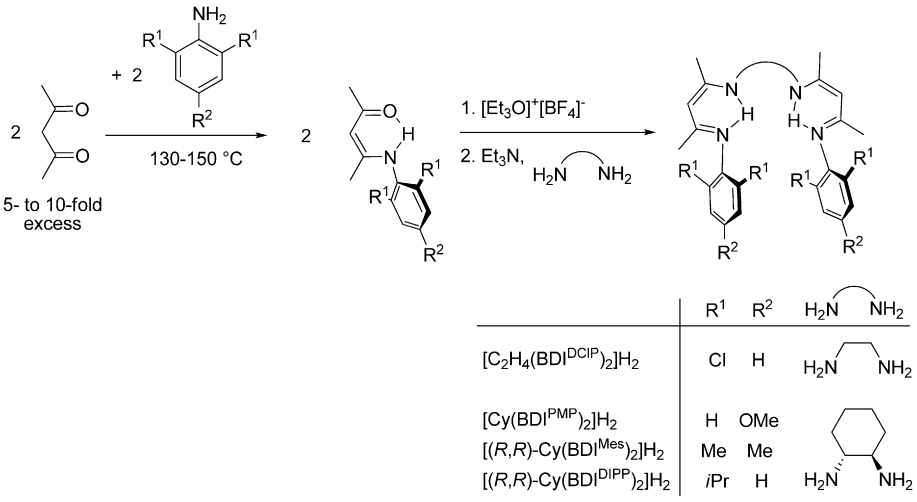

Scheme 1.

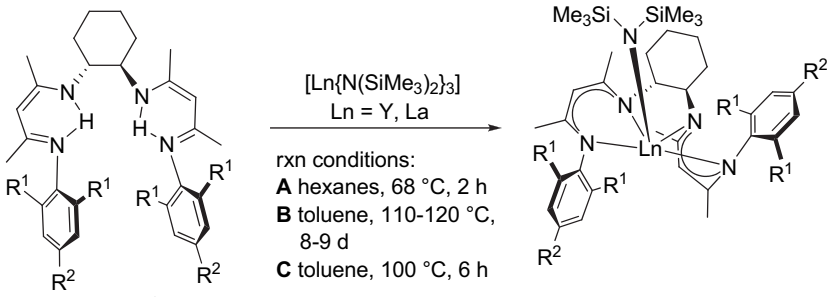

	R^1	R^2
[*rac*-Cy(BDI^{PMP})$_2$]H$_2$	H	OMe
[(*R*,*R*)-Cy(BDI^{Mes})$_2$]H$_2$	Me	Me
[(*R*,*R*)-Cy(BDI^{DIPP})$_2$]H$_2$	*i*Pr	H

	Ln	R^1	R^2	cond.
rac-**2**	La	H	OMe	**A**
(*R*,*R*)-**3**	Y	Me	Me	**B**
(*R*,*R*)-**4**	La	Me	Me	**C**
(*R*,*R*)-**5**	La	*i*Pr	H	**B**

Scheme 3.

$SiCH_3$ groups of the amido ligand give rise of a single broad signal in the ^{1}H NMR spectrum, which is indicative of a slightly hindered rotation around the Y–N bond. These spectral features place the fluxionality of complex **3** between that of the sterically more hindered diisopropylphenyl-substituted lanthanum complex **5**, which displayed a C_1 symmetric structure on the NMR time scale in solution at room temperature, and the sterically more open mesityl-substituted lanthanum complex **4**, which displayed substantial fluxional behavior in solution at room temperature. A decoalescence of the signals in accordance with a C_1 symmetric structure was observed for **4** at −20 °C [10b]. As we will see later, the increase in fluxionality in the order **5** < **3** < **4** correlates well with a decline in the enantioselectivity in hydroamination/cyclization reactions of aminoalkenes.

The sterically less congested *p*-methoxyphenyl-substituted complex **2** displayed also fluxional behavior in solution. The ^{1}H NMR spectrum showed only one set of signals for both β-diketiminato moieties at 25 °C, but the resonances for the cyclohexyl methine protons were extremely broadened and practically undetectable at this temperature. The complex displayed a C_s symmetric structure on the NMR time scale at 80 °C. Decoalescence of the signals for the methine protons, the β-diketiminato methyl groups and the aromatic ring protons started at −10 °C. At −30 °C the ^{1}H NMR spectrum of the complex revealed the C_1 symmetric structure typical for cyclohexyl-linked complexes. Remarkably, the chemical shifts for the β-diketiminate methine hydrogens were very close to each other in **2** (4.63 and 4.61 ppm) in contrast to the large difference found in the spectra of 2,6-dialkylphenyl complexes (e.g. 5.10 and 4.14 ppm in **4** [10]), which can serve as an evidence for the considerable influence of the steric demand of the aromatic substituent on the overall ligand geometry.

X-ray crystallographic analyses of **3** and **4** are shown in Figs. 1 and 2, selected metrical parameters are tabulated in Table 1. The coordination geometry around the metal centers in **3** and **4** show strong resemblance to previously characterized cyclohexyl-linked bis(β-diketiminato) lanthanum complexes [10], in which the two β-diketiminato moieties and the amido ligand are coordinated in a distorted square pyramidal geometry. For the purpose of the catalytic studies presented later on in this study, we will focus primarily on the similarities and differences in the structures of **3** and **4**.

The N2-C-C-N3 torsion angle in **3** (−37.6(4)°) is smaller than in **4** (−40.3(3)°) or any other previously characterized cyclohexyl-linked lanthanum complex (41.5–44.1° [10]) or ethylene-linked complex (49.3–53.1° [10]). In order to minimize steric interactions in the complex, the two β-diketiminato moieties are almost orthogonal oriented to each other with an angle of 81.0° (in **3**), respectively 82.8° (in **4**), between the N_2C_2 planes. The two aromatic substituents are oriented in a *transoid* fashion, with one aromatic substituent pointing away from the amido group and the other aromatic substituent pointing towards the amido group. Both β-diketiminato moieties in complexes **3** and **4** are bound in an η^5 bonding mode, with the metal being displaced by 1.38–1.42 Å (in **3**), respectively 1.84–1.88 Å (in **4**), out of the N_2C_3 planes and short Ln···C contacts. Remarkably, the Ln···C contacts are slightly closer in **4** (2.98–3.13 Å) than in **3** (3.04–3.30 Å), despite the larger ionic radius of lanthanum in **4** in comparison to yttrium in **3**.

Due to the larger ionic radius of lanthanum, the front quadrant in lanthanum complex **4** is more open (described by N1–La–N4 = 132.01(7)°) in comparison to yttrium complex **3**

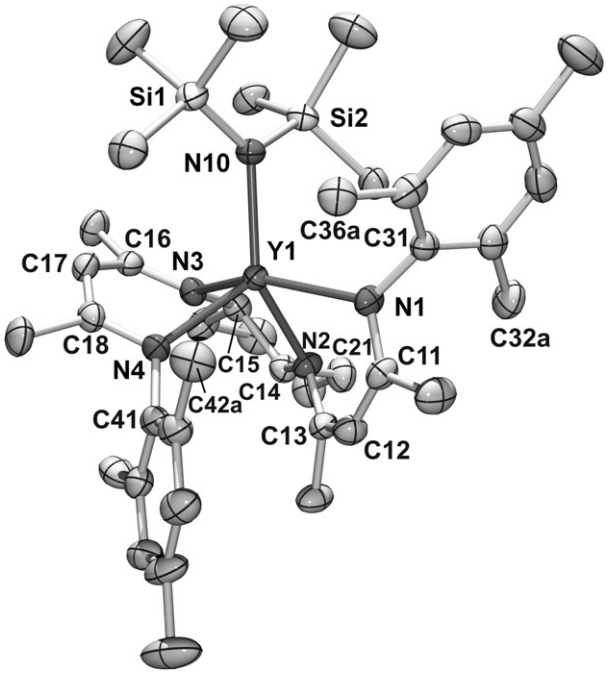

Fig. 1. ORTEP diagram of the molecular structure of *rac*-**3**. Thermal ellipsoids are drawn at the 50% probability level. Hydrogen atoms have been omitted for the sake of clarity.

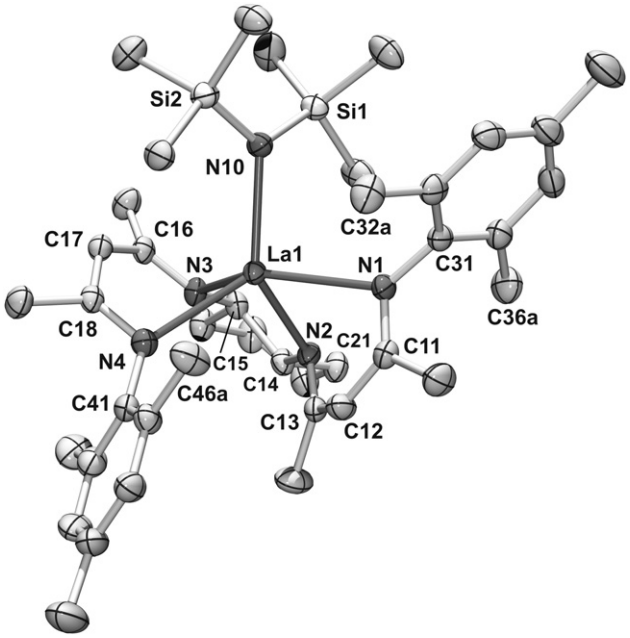

Fig. 2. ORTEP diagram of the molecular structure of *rac*-**4**. Thermal ellipsoids are drawn at the 50% probability level. Hydrogen atoms have been omitted for the sake of clarity.

(N1–Y–N4 = 115.34(12)°). Additionally, the N1–Ln–N3 angle in **3** (145.62(12)°) is larger in comparison to **4** (134.00(7)°), which suggests a more accessible back side in the yttrium complex **3** (*vide infra*).

Table 1
Selected bond lengths [Å], atomic distances [Å] and angles [°] for *rac*-**3** and *rac*-**4**.

	rac-**3** (Ln = Y)	*rac*-**4** (Ln = La)
Ln–N1	2.341(3)	2.545(2)
Ln–N2	2.344(3)	2.465(2)
Ln–N3	2.309(3)	2.450(2)
Ln–N4	2.295(3)	2.503(2)
Ln–N10	2.288(3)	2.424(2)
Ln···Si2	3.3413(11)	3.572(2)
Ln···Si1	3.5661(13)	3.591(2)
Ln···C11	3.137(3)	3.105(3)
Ln···C12	3.298(3)	3.068(3)
Ln···C13	3.087(3)	2.976(3)
Ln···C16	3.041(4)	3.021(3)
Ln···C17	3.209(3)	3.134(3)
Ln···C18	3.067(3)	3.117(3)
N1–Ln–N2	78.31(11)	72.77(7)
N1–Ln–N3	145.62(12)	134.00(7)
N1–Ln–N4	115.34(12)	132.01(7)
N1–Ln–N10	102.31(12)	94.20(7)
N2–Ln–N3	68.55(11)	64.40(7)
N2–Ln–N4	96.04(12)	97.51(7)
N2–Ln–N10	135.73(11)	129.15(7)
N3–Ln–N4	78.05(12)	71.69(7)
N3–Ln–N10	95.38(12)	99.81(7)
N4–Ln–N10	121.56(12)	124.25(7)
Ln–N10–Si1	125.60(18)	119.59(11)
Ln–N10–Si2	112.78(16)	118.62(11)
Si1–N10–Si2	121.25(19)	121.78(12)
N2–C–C–N3	−37.6(4)	−40.3(3)
C11–N1···C31···C32	71.2(5)	−94.8(3)
C11–N1–C31–C36	−112.6(4)	88.2(3)
C18–N4–C41–C42	−110.4(5)	72.0(3)
C18–N4–C41–C46	73.9(5)	−111.4(3)
Distances of Ln from N_2C_2 planes		
Ln···Plane(1)	1.384	1.880
Ln···Plane(2)	1.424	1.844
∠(Plane(1)/Plane(2))	81.0	82.8

Plane(1) = N1–C11–C13–N2, Plane(2) = N3–C16–C18–N4.

2.2. Catalytic hydroamination/cyclization

The catalytic activity of the bis(β-diketiminato) rare-earth metal complexes was examined in hydroamination/cyclization reactions of aminoalkenes (Table 2).

The structure of the linker unit in the bis(β-diketiminato) complexes has considerable influence on the steric properties of the complexes, but resulted only in minor effects on the catalytic activity. Thus, the cyclohexyl- and ethylene-linked lanthanum complexes **2**, **4**, and [{C_2H_4(BDI^{Mes})$_2$}LaN(SiMe$_3$)$_2$] (**8**) (Fig. 3) performed the cyclization of **6a** with similar activity at 25 °C (Table 2, entries 2, 4 and 7), however, the 2,6-dichlorophenyl-substituted complex **1** was completely inactive under the same reaction conditions. In agreement with the activating effect of larger *gem*-dialkyl substituents in the substrate [17], the cyclizations of **6b** and **6c** proceed much faster than the reaction of **6a**.

For a comparison, we also tested the sterically much less hindered mono(β-diketiminato) complexes [(BDI)La{N(SiMe$_2$X)$_2$}$_2$] (BDI = MesNC(Me)CHC(Me)NMes; X = Me (**9a**), H (**9b**)) (Fig. 3) [10b] in the catalytic cyclization of **6a**. While the bis(trimethylsilyl) amido complex **9a** reacted readily at 25 °C with high activity, the analogous bis(dimethylsilyl)amido complex **9b** reacted sluggish at 25 °C and appreciable activity was observed only at 60 °C (Table 2, entry 8 vs. entry 9). As noted earlier, this observation is in

Table 2
Hydroamination reactions catalyzed by β-diketiminato lanthanum and yttrium complexes.[a]

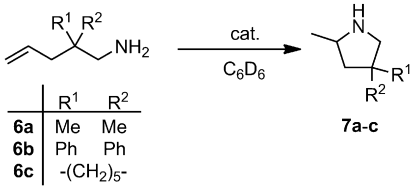

Entry	Substrate	Product	Cat.	(mol %)	*T* (°C)	N_t (h^{-1})[b]	%ee (config.)[c]
1			**1**	2.9	25	nr	–
2			*rac*-**2**	3	25	2.0	–
3			(*R*,*R*)-**3**	4.3	60	0.2	25 (*S*)
4			(*R*,*R*)-**4**	3.2	25	1.7	11 (*R*)
5			(*R*,*R*)-**5**	9.6	25	0.2	76 (*R*)
6	**6a**	**7a**	(*R*,*R*)-**5**	2.6	60	2.1	64 (*R*)
7			**8**	3.0	25	2.6	–
8			**9a**	4.3	25	22.3	–
9			**9b**	4.7	60	2.9	–
10			(*R*,*R*)-**3**	3.5	60	2.6	11 (*S*)
11			(*R*,*R*)-**4**	3.0	25	36.4	11 (*R*)
12			(*R*,*R*)-**4**	1.5	25	50	14 (*R*)
13			(*R*,*R*)-**5**	3.5	25	2.7	61 (*R*)
14	**6b**	**7b**	(*R*,*R*)-**5**[d]	2.7	25	2.9	64 (*R*)
15			(*R*,*R*)-**3**	3.0	60	2.6	42 (*S*)
16			(*R*,*R*)-**4**	2.6	25	26	5 (*R*)
17	**6c**	**7c**	(*R*,*R*)-**5**	3.0	25	2.3	53 (*R*)
18			**8**	3.0	25	32	–

[a] Reaction conditions: 3–10 mol% cat., C_6D_6, Ar atm., >95% conversion.
[b] N_t calculated from first half life.
[c] Enantiomeric excess determined by ^{19}F NMR spectroscopy of the Mosher amides of the corresponding pyrrolidine products. The absolute configuration of the hydroamination products was assigned based on ^{19}F NMR spectroscopic data of the Mosher amides reported in Ref. [8d].
[d] Added 33 equiv of THF relative to catalyst. nr = no reaction observed.

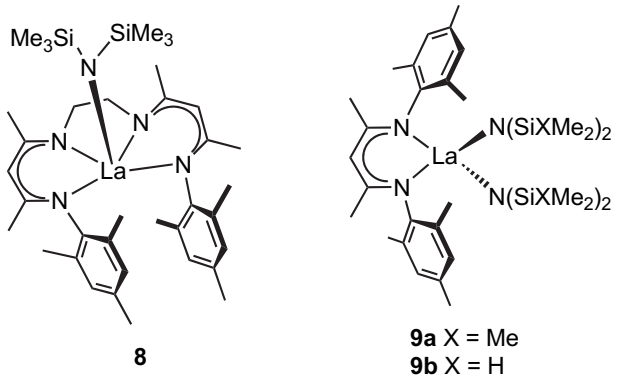

Fig. 3. Additional β-diketiminato lanthanum complexes [10] studied in catalytic hydroamination/cyclization reactions of aminoalkenes.

agreement to previous studies [7b,15], in which the low activity of bis(dimethylsilyl)amido complexes was ascribed to incomplete catalyst activation as a result of the lower basicity of this amido group in comparison to the bis(trimethylsilyl)amido ligand.

Catalytic experiments performed with chiral catalysts (*R*,*R*)-**3**, (*R*,*R*)-**4** and (*R*,*R*)-**5** indicated that the enantioselectivity of these systems is very sensitive to the identity/size of the rare-earth metal and the steric demand of alkyl groups in 2,6-positions of the aromatic substituents.

The methyl groups of a mesityl substituent are interacting insufficiently with the substrate for effective transfer of stereochemical information. The reaction of **6a-c** catalyzed by (*R*,*R*)-**4** gave preferentially the (*R*)-pyrrolidine in low enantioselectivity (Table 2, entries 4, 11, 12, and 16). Switching from lanthanum in (*R*,*R*)-**4** to yttrium in (*R*,*R*)-**3** improved the stereoselectivities slightly for **6a** (25% ee; Table 2, entry 3) and for **6c** (42% ee; Table 2, entry 15), however, the yttrium complex was less reactive and the reaction had to be performed at 60 °C. Interestingly, the yttrium complex (*R*,*R*)-**3** produced the (*S*)-enantiomer, while both lanthanum complexes (*R*,*R*)-**4** and (*R*,*R*)-**5** favor the (*R*)-enantiomer.

The increased steric demand of the bulky 2,6-diisopropylphenyl moiety in the lanthanum complex (*R*,*R*)-**5** improved the enantioselectivity significantly to 76% ee for **6a** (Table 2, entry 5), 61% ee for **6b** (Table 2, entry 13), and 53% ee for **6c** (Table 2, entry 17). However, this selectivity resulted also in a significant drop in reactivity when comparing (*R*,*R*)-**4** and (*R*,*R*)-**5** (Table 2, entries 4, 11, 16 vs. entries 5, 13, 17). The temperature dependence of the enantioselectivity seems to be slightly greater for (*R*,*R*)-**5** (Δee ≈ 3.4% ee/10 °C in the range of 25–60 °C; Table 2, entries 5 and 6), in comparison to binaphtholate rare-earth metal complexes (Δee ≈ 1.5% ee/10 °C in the range of 0–60 °C [8d]), potentially as a result of the greater fluxionality of the linked bis(β-diketiminato)-ligand framework. Addition of a 33-fold excess of THF (with respect to the catalyst) did not significantly diminish catalytic activity, but led to a slight increase in enantioselectivity (Table 2, entry 13 vs. 14).

NMR spectroscopic analysis of the catalytic reaction mixture in the cyclization of **6b** with (*R*,*R*)-**5** indicated a slow catalyst activation. With most catalysts, protonolysis of the bis(trimethylsilyl) amido group by the aminoalkene substrate is rapid and takes place immediately after mixing of the components. In the case of complex (*R*,*R*)-**5** the metal center seems to be strongly sterically encumbered by the auxiliary ligand, resulting in a decreased rate of catalyst activation (Fig. 4). The reaction showed an induction period at the beginning (≤2 h), which was then followed by a zero order rate dependence on substrate concentration until 90% conversion.

Another interesting point here is the form of the kinetic plots for the cyclization of **6b** catalyzed by (*R*,*R*)-**4** and (*R*,*R*)-**5**. While the

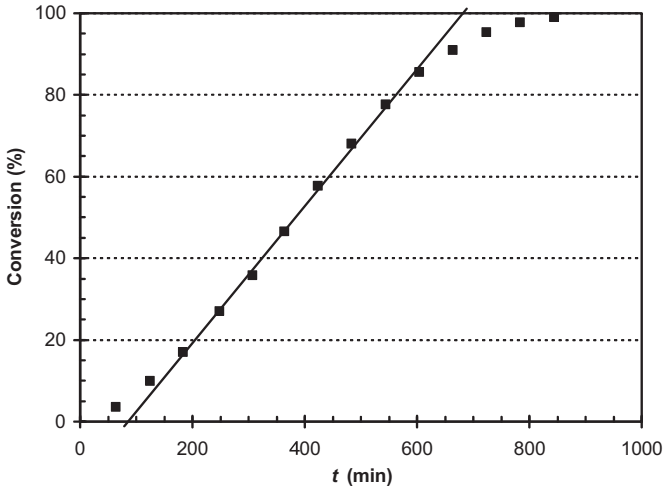

Fig. 4. Conversion of the substrate as a function of time for the hydroamination/cyclization of **6b**, using (*R*,*R*)-**5** in C_6D_6 at 25 °C. The line represents the least-square fit to the linear part of the data.

reaction mediated by the sterically more encumbered complex (*R*,*R*)-**5** displayed zero order rate dependence on substrate concentration for three half lifes (Fig. 4), the process catalyzed by (*R*,*R*)-**4** showed deviation from the linearity after approximately one half life (Fig. 5). This observation is in agreement to previous studies [5a–d,8e] that sterically more open catalysts are prone to product inhibition. In order to verify this hypothesis, a second batch of substrate **6b** was introduced to the catalytic system after the cyclization of the first batch was finished. Kinetic plots of both reactions clearly indicate more pronounced deviation for the second catalytic cycle, as well as a depressed reaction rate.

As noted above, the catalytic efficiency of the present β-diketiminato complexes was strongly affected by steric factors such as ionic radius of the metal and the steric bulk of the aryl substituents, which is an indication for highly steric encumbered catalytic species. The enantioselectivity is expected to arise from non-

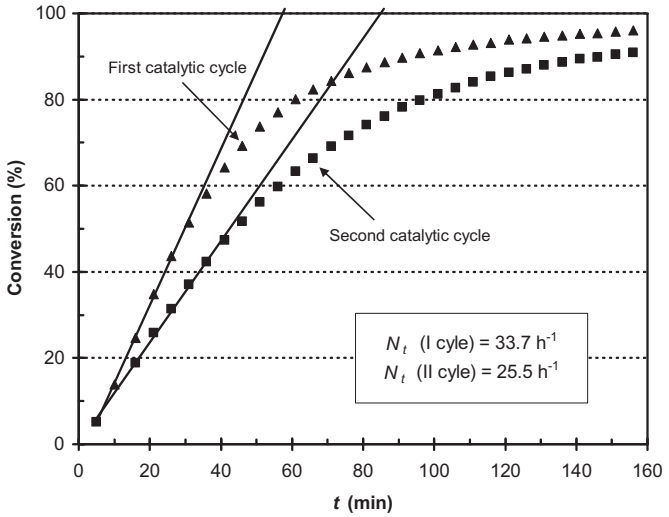

Fig. 5. Conversion of substrate as a function of time for the hydroamination/cyclization of **6b**, using (*R*,*R*)-**4** (3 mol% in first catalytic cycle) in C_6D_6 at 25 °C. Upon complete consumption of the first batch of substrate, a second cycle was started by introducing an additional aliquot of **6b**. The lines represent least-squares fit to the linear part of the data.

bonding interactions in the transition state of the rate-limiting insertion of the double bond into the Ln–N bond. The experimental results showed a significant increase in the enantiomeric excess for complex (*R*,*R*)-**5** (53–76% ee) in comparison to complex (*R*,*R*)-**4** (5–14% ee), revealing the significant influence of the aryl groups in these interactions. Another remarkable observation is the reversal of the product configuration in going from lanthanum to the smaller yttrium. The latter could result from a different approach of the substrate molecule to the metal center and/or different geometry of the ligand and consequently different steric interactions between the substrate and the supporting ligand. Presumably, the combination of the smaller ionic radius of Y^{3+} and the relatively high steric demand of the linked bis(β-diketiminato) ligands lead to an overcrowded complex structure, which behaves differently in comparison to the lanthanum complex. The crystallographic data of **3** and **4** revealed some differences in the geometry of the ancillary ligand around the metal. Similar effects have been noted for lanthanocene complexes, where an increase in enantioselectivity was observed in the lanthanide series going from La^{3+}- through the smaller Sm^{3+}-complex, with the enantioselectivity decreasing thereafter and ultimately favoring the opposite product antipode for Lu^{3+} [5b].

Analysis of the crystal structures of the catalysts amido precursors supports a reasonable model explaining the different behavior of the lanthanum and yttrium complexes. As shown in Fig. 6 (top), the cleft between the two mesityl substituents is significantly diminished in yttrium complex **3** compared to lanthanum complex **4** (3.738 Å vs. 4.292 Å). On the other hand, the rear side of the complexes also has a sizable cleft as depicted in Fig. 6 (bottom), with a slightly larger gap for the yttrium complex **3** in comparison to the lanthanum complex **4** (4.887 Å vs. 4.834 Å). The increase in the gap at the rear side is apparently limited by the steric restraints inherent to the linked bis(β-diketiminato) ligand framework.

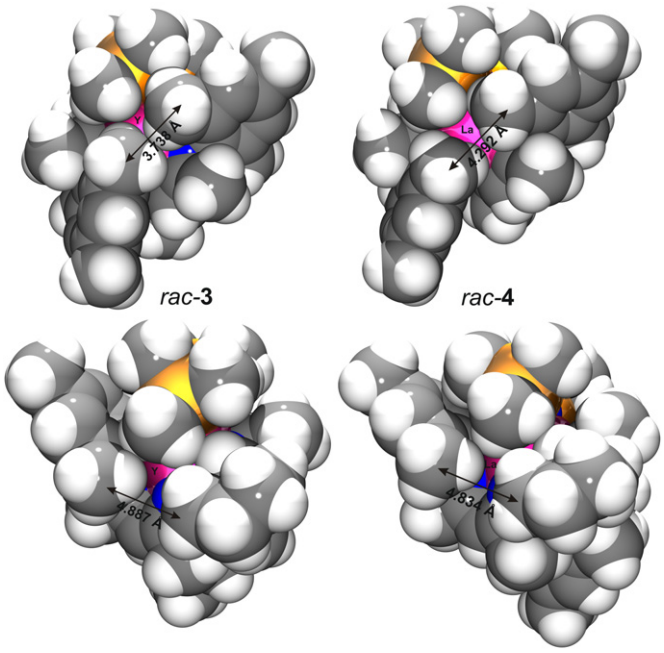

Fig. 6. Space filling representation of the structure of *rac*-**3** (left) and *rac*-**4** (right). The front view (top) shows the cleft for the frontal approach of the substrate, as defined by the distance between the methyl groups of the two mesityl moieties (C36a···C42a = 3.738 Å in *rac*-**3**, C32a···C46a = 4.292 Å in *rac*-**4**). The rear view (bottom) shows the cleft for a potential approach of the substrate from the rear, as defined by the distance between one of the mesityl methyl groups and the cyclohexyl backbone (C32a···C21 = 4.887 Å in *rac*-**3**, C36a···C21 = 4.834 Å in *rac*-**4**).

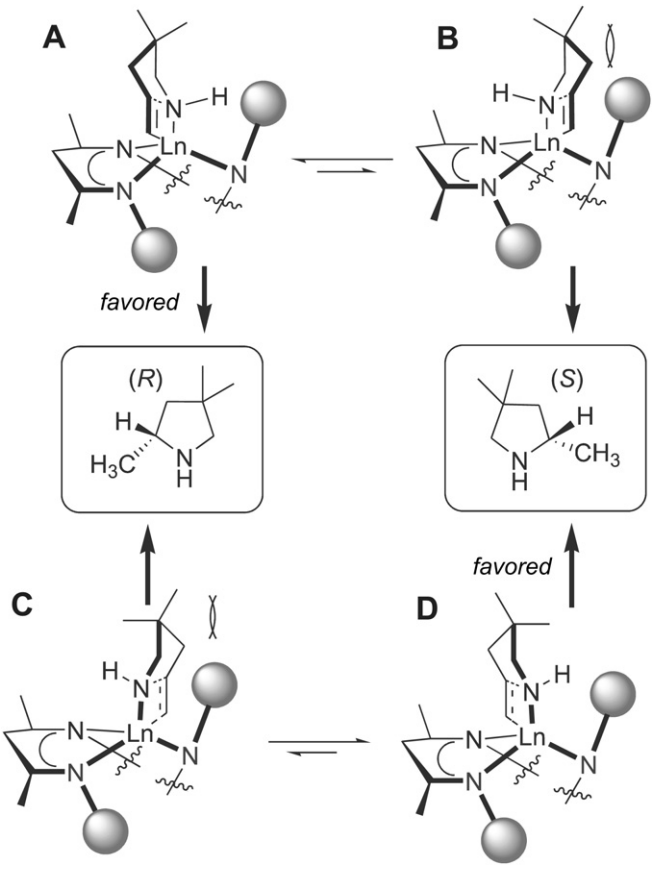

Fig. 7. Stereochemical models for intramolecular hydroamination/cyclization of 2,2-dimethyl-pent-4-enylamine (**6a**) catalyzed by (*R*,*R*)-**3** and (*R*,*R*)-**4**. The drawings show an equatorial approach of the alkene to the Ln-amido bond from different sides — frontal in case of the La-complex (**A** and **B**) and from the rear side in case of the Y-complex (**C** and **D**), which could rationalize the observed reversal in the absolute product configuration.

Therefore, the front side of yttrium complex **3** is sterically significantly more hindered than in lanthanum complex **4**. With the frontal approach blocked, the more open coordination space on the rear side of complex **3** is presumably better accessible for an approach of the alkene moiety from that side. As shown in Fig. 7, the approach of the alkene to the Ln-amido bond from the rear favors the opposite enantiotopic face of the double bond in the cyclization transition state. The present model is also in accordance with the role of the 2,6-dialkylphenyl-substituents, since a more demanding 2,6-diisopropylphenyl group will interact more effectively than a mesityl group.

3. Conclusion

Herein we have reported the synthesis and catalytic application of a variety of linked bis(β-diketiminato) rare-earth metal complexes. The complexes displayed good to moderate catalytic activity in the hydroamination/cyclization of aminoalkenes depending on the steric hindrance around the metal center. The sterically most demanding and most rigid diisopropylphenyl-substituted complex (*R*,*R*)-**5** displayed significantly higher enantioselectivities but lower catalytic activity in comparison to the sterically more open and more fluxional mesityl-substituted complex (*R*,*R*)-**4**. The smaller yttrium metal center in complex (*R*,*R*)-**3** led to reduced activity as well as a reversal in enantioselectivity, which may be rationalized by a change of the approach of

the alkene moiety to the Ln-amido bond in the cyclization transition state.

4. Experimental

4.1. General procedures

All operations were performed under an inert atmosphere of nitrogen or argon using standard Schlenk-line or glovebox techniques. After drying over KOH, THF was distilled from sodium benzophenone ketyl. Hexanes, pentane and toluene were purified by distillation from sodium/triglyme benzophenone ketyl. Anhydrous YCl_3 (Aldrich) and $LaCl_3$ (Strem) were used as received. [Ln{N(SiMe$_3$)$_2$}$_3$] (Ln = Y, La) [18], 2-(2,4,6-trimethylphenyl)-aminopent-2-en-4-one [10], 4-((2,6-diisopropylphenyl)amino)pent-3-en-2-one [10], 2,2-dimethyl-pent-4-enylamine (**6a**) [3f,19], 2,2-diphenyl-pent-4-enylamine (**6b**) [3f,7c], and *C*-(1-allyl-cyclohexyl)-methylamine (**6c**) [3f,20] were synthesized as described in the literature. The racemic complexes [{Cy(BDI^{Mes})$_2$}LaN(SiMe$_3$)$_2$] (**4**), [{Cy(BDI^{DIPP})$_2$}LaN(SiMe$_3$)$_2$] (**5**), as well as complexes [{C$_2$H$_4$(BDI^{Mes})$_2$}LaN(SiMe$_3$)$_2$] (**8**) and [(BDI)LnN(SiXMe$_2$)$_2$] (BDI = MesNC(Me)CHC(Me)NMes; X = Me (**9a**), H (**9b**)) were prepared as reported previously [10]. Enantiomerically enriched (≥98% ee) *trans*-(*R*,*R*)-1,2-diaminocyclohexane was obtained from the *L*-(+)-tartrate salt, after hydrolysis with 20% solution of NaOH [21]. (*R*)-(+)-α-Methoxy-α-trifluoromethylphenylacetic acid (>99% ee, from Reuter Chemische Apparatebau KG (RCA), Freiburg, Germany) was transformed to its acid chloride using oxalyl chloride/DMF in hexanes [22]. All other chemicals were commercially available and used as received. ^{1}H, ^{13}C and ^{19}F NMR spectra were recorded on Bruker Avance 300 or Avance 400 spectrometer. The enantiomeric excess of the hydroamination/cyclization reactions were determined via ^{19}F NMR spectroscopy of the Mosher amides as described earlier [3f,8d].

4.2. 4-((p-Methoxyphenyl)amino)-pent-3-en-2-one

2,4-Pentadione (84.134 g, 840 mmol) and *p*-methoxyaniline (19.51 g, 158.4 mmol) were added to a 250 mL round-bottom flask equipped with a stir bar. A simple distillation apparatus was attached to collect water and the neat solution was heated to 130–140 °C for 24 h. The excess of 2,4-pentadione was removed *in vacuo*, and the residue was distilled under vacuum (94–101 °C, 0.2 mmHg) to give a yellowish liquid, which solidified at −20 °C. Washing with hexanes and drying *in vacuo*, produced the title compound in 97% (31.7 g) yield. ^{1}H NMR (400 MHz, $CDCl_3$): δ = 12.26 (br s, 1H, NH), 7.00 (2 overlapping dd, $^3J_{H,H}$ = 8.8 Hz, $^4J_{H,H}$ = 2.6 Hz, 2H, 2,6-C$_6$H$_4$), 6.84 (2 overlapping dd, $^3J_{H,H}$ = 8.8 Hz, $^4J_{H,H}$ = 2.6 Hz, 2H, 3,5-C$_6$H$_4$), 5.12 (s, 1H, β-CH), 3.77 (s, 3H, OCH$_3$), 2.06 (s, 3H, CH$_3$), 1.87 (s, 3H, CH$_3$); ^{13}C{^{1}H} NMR (100.6 MHz, $CDCl_3$): δ = 195.8 (CO), 161.2 (CH$_3$*C*N), 157.7 (4-C$_6$H$_4$), 131.5 (aryl-C$_{ipso}$), 126.6 (2,2′-C$_6$H$_4$), 114.2, (3,3′-C$_6$H$_4$), 96.8 (β-CH), 55.4 (OCH$_3$), 29.0, 19.6 (CH$_3$).

4.3. 4-((2,6-Dichlorophenyl)amino)-pent-3-en-2-one

A mixture of 2,6-dichloraniline (4.07 g, 25.12 mmol), 2,4-pentadione (10-fold excess, 25.1 g, 251 mmol) and *p*-toluenesulfonic acid (3.95 g, 20 mmol) was refluxed for 24 h in a Dean-Stark apparatus. After removing the excess of pentadione a brown liquid product was obtained. Distillation *in vacuo* gave a pale yellow solid, which was crystallized from a hexanes/methanol-mixture (5:1) at −20 °C. The aimed compound was obtained in 29% yield (1.761 g). ^{1}H NMR (400 MHz, $CDCl_3$): δ = 12.03 (br s, 1H, NH), 7.35 (d, $^3J_{H,H}$ = 8.1 Hz, 2H, C$_6$H$_3$), 7.17 (pt, $^3J_{H,H}$ = 8.1 Hz, 1H, C$_6$H$_3$), 5.28 (s, 1H, β-CH), 2.11 (s, 3H, CH$_3$), 1.71 (s, 3H, CH$_3$); ^{13}C{^{1}H} NMR (100.6 MHz, $CDCl_3$): δ = 197.2 (CO), 161.3 (CH$_3$CN), 135.0 (4-C$_6$H$_3$), 134.6 (aryl-C$_{ipso}$), 128.7 (2,2′-C$_6$H$_3$), 128.4 (3,3′-C$_6$H$_3$), 97.3 (β-CH), 29.3, 19.0 (CH$_3$).

4.4. [C$_2$H$_4$(BDI^{DClP})$_2$]H$_2$

A solution of [Et$_3$O]$^+$[BF$_4$]$^-$ (1.578 g, 8.31 mmol) in CH_2Cl_2 (10 mL) was slowly added to a solution of 4-((2,6-dichlorophenyl)-amino)-pent-3-en-2-one (1.736 g, 7.11 mmol) in CH_2Cl_2 (15 mL) under an atmosphere of nitrogen. The mixture was stirred for 3 h at room temperature. Then Et$_3$N (0.8 g, 7.9 mmol) was added and the mixture was stirred for another 5 min. Ethylenediamine (0.253 g, 4.21 mmol) in Et$_3$N (5 mL) was added to the mixture and the stirring was continued overnight. The solvent was removed *in vacuo*. The product was extracted with toluene (3 × 25 mL). After removing the solvent *in vacuo* the residue was treated with MeOH and kept in a fridge at −20 °C. The desired compound was obtained as a white solid in 60% yield (1.094 g) after filtration and washing with MeOH. ^{1}H NMR (400 MHz, C$_6$D$_6$): δ = 10.54 (br s, 2H, NH), 7.12 (d, $^3J_{H,H}$ = 8 Hz, 4H, C$_6$H$_3$), 6.40 (t, $^3J_{H,H}$ = 8.0 Hz, 2H, C$_6$H$_3$), 4.59 (s, 2H, β-CH), 2.54 (m, 4H, CH$_2$), 1.69 (s, 6H, CH$_3$), 1.63 (s, 6H, CH$_3$); ^{13}C{^{1}H} NMR (100.6 MHz, C$_6$D$_6$): δ = 168.9, 157.7 (CH$_3$CN), 147.4 (aryl-C$_{ipso}$), 123.1, 128.2 (aryl), 94.2 (β-CH), 44.3 (CH$_2$), 21.2, 19.3 (CH$_3$). Anal. Calcd for C$_{24}$H$_{26}$N$_4$Cl$_4$ (512.308): C, 56.27; H, 5.12; N, 10.94. Found: C, 56.09; H, 5.02; N, 10.79.

4.5. [Cy(BDI^{PMP})$_2$)$_2$]H$_2$

A solution of [Et$_3$O]$^+$[BF$_4$]$^-$ (4.201 g, 22.11 mmol) in CH_2Cl_2 (10 mL) was slowly added to a solution of 4-((*p*-methoxyphenyl) amino)-pent-3-en-2-one (4.105 g, 20.00 mmol) in CH_2Cl_2 (15 mL) under a nitrogen atmosphere. The mixture was stirred for 3 h at room temperature. Then Et$_3$N (2.8 mL, 20 mmol) was added and the mixture was stirred for another 5 min. Racemic *trans*-1,2-diaminocyclohexane (1.213 g, 10.62 mmol) in Et$_3$N (10 mL) was added to the mixture and the stirring was continued overnight. The solvent was removed *in vacuo*. The product was extracted with pentane (3 × 25 mL). After removing the solvent, the residue was dissolved in MeOH and stored in a fridge at −20 °C. Crystallization afforded [Cy(BDI^{PMP})$_2$)$_2$]H$_2$ in form of white crystals, which were filtered off, washed with hexanes and dried *in vacuo* to give 0.741 g (15%) of spectroscopically pure product. ^{1}H NMR (400 MHz, C$_6$D$_6$): δ = 11.46 (br s, 2H, NH), 6.86 (s, 8H, C$_6$H$_4$), 4.67 (s, 2H, β-CH), 3.30 (s, 6H, OCH$_3$), 3.02 (br m, 2H, ring-CH), 1.91 (s, 6H, CH$_3$), 1.81 (s, 6H, CH$_3$), 1.78 (br m, 2 H, ring-CH$_2$), 1.38 (br m, 2 H, ring-CH$_2$), 1.10 (br m, 2 H, ring-CH$_2$), 0.90 (br m, 2 H, ring-CH$_2$); ^{13}C{^{1}H} NMR (100.6 MHz, C$_6$D$_6$): δ = 166.4 (4-C$_6$H$_4$), 155.9, 155.7 (CH$_3$*C*N), 145.5 (aryl-C$_{ipso}$), 122.8, 114.5 (aryl), 94.9 (CH), 58.1 (ring-CH), 55.0 (OCH$_3$), 33.2, 24.3 (ring-CH$_2$), 21.1, 19.4 (CH$_3$). Anal. Calcd for C$_{30}$H$_{40}$N$_4$O$_2$ (488.66): C, 73.74; H, 8.25; N, 11.47. Found: C, 73.64; H, 8.26; N, 11.69.

4.6. [(R,R)-Cy(BDI^{Mes})$_2$]H$_2$

The enantiopure ligand was synthesized in a procedure analogous to that for the racemic compound [10]. A solution of [Et$_3$O]$^+$[BF$_4$]$^-$ (4.250, 22.37 mmol) in CH_2Cl_2 (20 mL) was slowly added to a solution of 2-(2,4,6-trimethylphenyl)-aminopent-2-en-4-one (4.382 g, 20.16 mmol) in CH_2Cl_2 (10 mL) under a nitrogen atmosphere. The mixture was stirred for 2.5 h at room temperature. Et$_3$N (2.8 mL, 20 mmol) was added to the clear pale yellow solution and the mixture was stirred for another 5 min. Then *trans*-(*R*,*R*)-1,2-diaminocyclohexane (1.14 g, 10 mmol) in Et$_3$N (10 mL) was added to the mixture and the stirring was continued overnight. Volatiles were removed *in vacuo* and the residue was extracted with pentane (2 × 20 mL) and toluene (20 mL). [NEt$_3$H]$^+$[BF$_4$]$^-$ was separated as

an oily precipitate. Toluene was removed *in vacuo* and the residue was dissolved in EtOH. Crystallization at −20 °C afforded 1.481 g (29%) of [(*R*,*R*)-Cy(BDI^{Mes})$_2$]H$_2$. The spectroscopic data of the product were identical with the data of the racemic compound [10].

4.7. [(*R*,*R*)-Cy(BDI^{DIPP})$_2$]H$_2$

A 100 mL Schlenk flask was charged with 4-((2,6-diisopropylphenyl)-amino)-pent-2-en-3-one (3.900 g, 15.04 mmol). This was dissolved in CH_2Cl_2 (10 mL) and a solution of $[Et_3O]^+[BF_4]^-$ (3.135 g, 16.50 mmol) in CH_2Cl_2 (20 mL) was slowly added under a nitrogen atmosphere. After stirring for 3 h at room temperature Et_3N (2.1 mL, 15 mmol) was added slowly. The mixture was stirred for another 15 min and then *trans*-(*R*,*R*)-1,2-diaminocyclohexane (0.856 g, 7.50 mmol) in Et_3N (10 mL) was added to the mixture. After stirring at room temperature for 18 h, the volatiles were removed *in vacuo* and the residue was treated with pentane (3 × 15 mL) and subsequently toluene (2 × 25 mL) to extract the product. Finally, crystallization from MeOH at −20 °C afforded [(*R*,*R*)-Cy(BDI^{DIPP})$_2$]H$_2$ in 34% yield (1.521 g). The spectroscopic data of the product were identical with those of the racemic compound [10].

4.8. [{C$_2$H$_4$(BDI^{DClP})$_2$}LaN(SiMe$_3$)$_2$] (**1**)

A Schlenk flask was charged with [C$_2$H$_4$(BDI^{DClP})$_2$]H$_2$ (512.3 mg, 1.00 mmol) and [La{N(SiMe$_3$)$_2$}$_3$] (620.1 mg, 1.00 mmol). Toluene (10 mL) was added and the reaction mixture was stirred at 65 °C for 3 h. The solvent and volatiles were removed *in vacuo*. A waxy material was obtained, which contained residual free amine and a small amount toluene. After addition of hexanes (10 mL) a white solid precipitated. All volatiles were removed *in vacuo* to give a pale yellow powder of **1** (796.7 mg, 98%), which was pure according to NMR spectroscopy. ^{1}H NMR (400 MHz, C_6D_6): $\delta = 6.85$ (dd, $^3J_{H,H} = 8.0$ Hz, $^4J_{H,H} = 1.4$ Hz, 4H, 3-C$_6$H$_3$), 6.25 (t, $^3J_{H,H} = 8.0$ Hz, 2H, 4-C$_6$H$_3$), 4.84 (s, 2H, β-CH), 3.74 (dt, $^2J_{H,H} = 13$ Hz, $^3J_{H,H} = 6.3$ Hz, 2H, CH$_2$), 3.21 (dt, $^2J_{H,H} = 13$ Hz, $^3J_{H,H} = 6.3$ Hz, 2H, CH$_2$), 1.67 (s, 6H, CH$_3$), 1.63 (s, 6H, CH$_3$), 0.34 (s, 18H, SiCH$_3$); ^{13}C{^{1}H} NMR (100.6 MHz, C_6D_6): $\delta = 165.0$, 160.5 (CH$_3$*C*N), 146.1 (aryl-C$_{ipso}$), 131.6, 131.2, 128.8, 123.7 (aryl), 100.0 (β-CH), 51.2 (CH$_2$), 24.3, 21.6 (CH$_3$), 4.4 (SiCH$_3$). Anal. Calcd for $C_{30}H_{42}N_5Cl_4LaSi_2$ (809.58): C, 44.51; H, 5.23; N, 8.65. Found: C, 44.38; H, 5.38; N, 8.24.

4.9. [{Cy(BDI^{PMP})$_2$}LaN(SiMe$_3$)$_2$] (**2**)

A Schlenk flask was charged with [Cy(BDI^{PMP})$_2$]H$_2$ (489.2 mg, 1.00 mmol) and [La{N(SiMe$_3$)$_2$}$_3$] (620.1 mg, 1.00 mmol). Hexanes (10 mL) were added and the reaction mixture was stirred at reflux (68 °C) for 2 h. The solvent and volatiles were removed *in vacuo*. A waxy material was obtained and addition of pentane (5 mL) caused precipitation of a white solid material. After filtration the residue was washed with additional pentane (5 mL). The solid product was dried *in vacuo* to give 531 mg, (68%) of **2**. ^{1}H NMR (400 MHz, C_6D_6, 80 °C): $\delta = 6.74$ (m, 4H, aryl), 6.51 (m, 4H, aryl), 4.63 (s, 2H, β-CH), 3.89 (m, 2H, ring-CH), 3.40 (s, 6H, OCH$_3$), 2.10 (m, 2H, ring-CH$_2$), 1.86 (s, 3H, CH$_3$), 1.77–1.75 (m, 2H, ring-CH$_2$), 1.71 (s, 6H, CH$_3$), 1.70 (m, 2H, ring-CH$_2$), 1.34 (m, 2H, ring-CH$_2$), 0.22 (s, 18H, SiCH$_3$); ^{13}C{^{1}H} NMR (100.6 MHz, C_6D_6, 80 °C): $\delta = 163.7$ (4-C$_6$H$_4$), 160.4, 157.8 (CH$_3$*C*N), 140.7 (aryl-C$_{ipso}$), 126.3, 116.1 (aryl), 99.3 (β-CH), 64.6 (ring-CH), 55.4 (OCH$_3$), 34.0, 26.5 (ring-CH$_2$), 23.3, 22.7 (CH$_3$), 4.8 (SiCH$_3$); ^{1}H NMR (400 MHz, toluene-d_8, −30 °C): $\delta = 6.64$ (d, $^3J_{H,H} = 9.6$ Hz, 2H, aryl), 6.68 (d, $^3J_{H,H} = 9.3$ Hz, 2H, aryl), 6.52 (d, $^3J_{H,H} = 8.6$ Hz, 2H, aryl), 6.24 (br m, 2H, aryl), 4.63 (s, 1H, β-CH), 4.61 (s, 1H, β-CH), 4.30 (dt, $^3J_{H,H} = 2.3$ Hz, $^3J_{H,H} = 10.8$ Hz, 1H, ring-CH), 3.39 (m, 1H, ring-CH), 3.15 (s, 6H, OCH$_3$), 2.14 (m, 1H, ring-CH$_2$), 1.89–1.83 (m, 2H, ring-CH$_2$), 1.80 (s, 3H, CH$_3$), 1.78 (m, 1H, ring-CH$_2$), 1.73 (s, 3H, CH$_3$), 1.67 (s, 6H, CH$_3$), 1.56 (m, 2H, ring-CH$_2$), 1.43 (m, 1H, CH$_2$), 1.10 (m, 1H, ring-CH$_2$), 0.34 (s, 9H, SiCH$_3$), 0.32 (s, 9H, SiCH$_3$); ^{13}C{^{1}H} NMR (100.6 MHz, toluene-d_8, −30 °C): $\delta = 165.1$, 162.1 (4-C$_6$H$_4$), 160.8, 158.9, 157.5, 157.0 (CH$_3$*C*N), 139.7, 139.4 (aryl-C$_{ipso}$), 126.8, 125.4 (2-C$_6$H$_4$), 115.8, 115.4 (3-C$_6$H$_4$), 101.1, 98.7 (β-CH), 65.3, 62.3 (ring-CH), 54.71, 54.66 (OCH$_3$), 34.8, 32.8 (ring-CH$_2$), 27.5, 25.6 (ring-CH$_2$), 24.3, 23.85, 23.82, 21.6 (CH$_3$), 4.9, 4.8 (SiCH$_3$). Anal. Calcd for $C_{36}H_{56}N_5LaO_2Si_2$ (785.95): C, 55.02; H, 7.18; N, 8.91. Found: C, 54.85; H, 7.16; N, 8.41.

4.10. [{(*R*,*R*)-Cy(BDI^{Mes})$_2$}YN(SiMe$_3$)$_2$] ((*R*,*R*)-**3**)

A Schlenk flask was charged with [(*R*,*R*)-Cy(BDI^{Mes})$_2$]H$_2$ (256.2 mg, 0.50 mmol) and [Y{N(SiMe$_3$)$_2$}$_3$] (285 mg, 0.50 mmol). Toluene (5 mL) and THF (74 mg, 1.0 mmol) were added and the mixture was stirred for 8 days at 120 °C. Volatiles were removed *in vacuo* to give a pale yellow powder of (*R*,*R*)-**3** in quantitative yield (372 mg, 98%), which was pure by NMR spectroscopy. The racemic complex was obtained in an analogous manner and gave identical ^{1}H and ^{13}C NMR spectra. ^{1}H NMR (400 MHz, C_6D_6): $\delta = 6.89$ (s, 1H, C$_6$H$_2$), 6.78 (s, 1H, C$_6$H$_2$), 6.76 (s, 1H, C$_6$H$_2$), 6.71 (s, 1H, C$_6$H$_2$), 5.97 (s, 1H, β-CH), 4.53 (m, 1H, ring-CH), 4.27 (s, 1H, β-CH), 3.10, (ddd, $^3J_{ax\text{-}ax} = 14$ Hz, $^3J_{ax\text{-}eq} = 3.6$ Hz, 1H, ring-CH), 2.56 (s, 3H, CH$_3$), 2.42 (m, 1H, ring-CH$_2$), 2.39 (s, 3H, CH$_3$), 2.19 (s, 3H, CH$_3$), 2.16 (s, 3H, CH$_3$), 2.03 (s, 3H, CH$_3$), 2.01 (s, 3H, CH$_3$), 1.77 (s, 3H, CH$_3$), 1.73 (m, 2H, ring-CH$_2$), 1.65 (m, 1H, ring-CH$_2$), 1.594 (s, 3H, CH$_3$), 1.590 (s, 3H, CH$_3$), 1.38 (s, 3H, CH$_3$), 1.50 (m, 1H, CH$_2$), 1.20–1.36 (m, 2H, ring-CH$_2$), 1.09 (m, 1H, CH$_2$), 0.1–0.6 (br s, 18H, SiCH$_3$); ^{13}C{^{1}H} NMR (100.6 MHz, C_6D_6): $\delta = 164.2$, 164.1, 163.5, 162.3 (CH$_3$*C*N), 147.4, 145.3 (aryl-C$_{ipso}$), 133.5, 132.92, 132.88, 132.80 (2C), 131.6 (2,4,6-C$_6$H$_2$), 130.0, 129.6, 129.4, 128.97 (3,5-C$_6$H$_2$), 101.8, 97.5, (β-CH), 69.9, 65.3 (ring-CH), 33.4, 33.1, 26.7, 25.4 (ring-CH$_2$), 25.3, 24.4, 24.0, 22.0, 21.6, 21.0 (3C), 18.9, 18.7 (CH$_3$), 5.8 (SiCH$_3$). Anal. Calcd for $C_{40}H_{64}N_5YSi_2$ (760.05): C, 63.21; H, 8.49; N, 9.21. Found: C, 63.12; H, 8.35; N, 8.61.

4.11. [{(*R*,*R*)-Cy(BDI^{Mes})$_2$}LaN(SiMe$_3$)$_2$] ((*R*,*R*)-**4**)

A Schlenk flask was charged with [(*R*,*R*)-Cy(BDI^{Mes})$_2$]H$_2$ (513 mg, 1.00 mmol) and [La{N(SiMe$_3$)$_2$}$_3$] (621.6 mg, 1.00 mmol). Toluene (10 mL) was added and the mixture was stirred for 6 h at 100 °C. All volatiles were removed *in vacuo* to give an orange powder of the product in quantitative yield. The ^{1}H NMR spectrum showed the presence of some impurities. Therefore, pentane (10 mL) was added and, after filtration, the clear solution was stored at −30 °C for crystallization. The mother liquor was decanted *via* cannula to leave 680 mg (84%) of (*R*,*R*)-**4** as white crystals. ^{1}H and ^{13}C NMR spectra of the complex were identical with those of the racemic compound [10].

4.12. [{(*R*,*R*)-Cy(BDI^{DIPP})$_2$}LaN(SiMe$_3$)$_2$] ((*R*,*R*)-**5**)

A Schlenk flask was charged with [(*R*,*R*)-Cy(BDI^{DIPP})$_2$]H$_2$ (569.6 mg, 1.0 mmol) and [La{N(SiMe$_3$)$_2$}$_3$] (620 mg, 1.0 mmol). Toluene (5 mL) was added and the mixture was stirred for 9 days at 110 °C. Volatiles were removed *in vacuo* to give a pale yellow foam-like product, which was dissolved in pentane (15 mL). After filtration volatiles were removed to give the title compound in 96% yield (863 mg), which was pure by NMR spectroscopy. ^{1}H and ^{13}C NMR are identical with those of the racemic compound [10].

4.13. X-ray crystal structure analysis of rac-**3** and rac-**4**

Clear, slight yellow plates of *rac*-**3**, $C_{40}H_{64}N_5Si_2Y$, 760.05 g mol^{-1}, were obtained from a cold hexanes solution at −35 °C. Crystal size

0.20 × 0.20 × 0.20 mm, orthorhombic, $P2_12_12_1$, $a = 11.698(2)$ Å, $b = 11.855(2)$ Å, $c = 30.412(6)$ Å, $V = 4217.5(15)$ Å^3, $Z = 4$, $D_{calc} = 1.197$ Mg/m^3, $\mu = 1.472$ mm^{-1}. Data were collected on a Nonius KappaCCD area detector at 173(2) K up to $2\theta_{max} = 55.0°$ (*Mo-Kα* radiation). 9431 reflections were collected for *rac*-**3**, 9431 were unique [R(int) = 0.0000] of which 7452 were observed [$I > 2\sigma(I)$]. $R_1 = 0.0478$, $wR_2 = 0.1323$ (obsd. data), goodness-of-fit on $F^2 = 1.044$; residual electron density (max/min) 0.426/−0.381 e Å^{-3}. Clear, slight yellow plates of *rac*-**4**, $C_{40}H_{64}LaN_5Si_2$, 810.05 g mol^{-1}, were obtained from a cold hexanes solution at −35 °C. Crystal size 0.20 × 0.20 × 0.20 mm, monoclinic, $P2_1/c$, $a = 13.0912(3)$ Å, $b = 11.9471(1)$ Å, $c = 27.3710(6)$ Å, $\beta = 96.318(1)°$, $V = 4254.88(14)$ Å^3, $Z = 4$, $D_{calc} = 1.265$ Mg/m^3, $\mu = 1.092$ mm^{-1}. Data were collected on a Nonius KappaCCD area detector at 173(2) K up to $2\theta_{max} = 55.0°$ (*Mo-Kα* radiation). 17,137 reflections were collected for *rac*-**4**, 9738 were unique [R(int) = 0.0283] of which 7684 were observed [$I > 2\sigma(I)$]. $R_1 = 0.0314$, $wR_2 = 0.0949$ (obsd. data), goodness-of-fit on $F^2 = 1.018$; residual electron density (max/min) 0.686/−0.681 e Å^{-3}. Cell parameters were obtained from 10 frames using a 10° scan and refined with 5013 reflections for *rac*-**3** and 8494 reflections for *rac*-**4**. Lorentz, polarization, and empirical absorption corrections were applied [23a,b]. The space group was determined from systematic absences and subsequent least-squares refinement. The structures were solved by direct methods. The parameters were refined with all data by full-matrix-least-squares on $F2$ using SHELXL-97 [23c]. Hydrogen atoms were fixed in idealized positions using a riding model. Non-hydrogen atoms were refined anisotropically. Scattering factors, and $\Delta f'$ and $\Delta f''$ values, were taken from literature [23d].

4.14. Typical NMR-scale catalytic hydroamination/cyclization reaction

In the glovebox, the appropriate substrate (ca. 0.25 mmol) was loaded into a screw cap NMR tube. C_6D_6 (0.5 mL) was added, followed by addition of the rare-earth metal catalyst precursor (3–10 mol%). The tube was then sealed and the reaction monitored by ^{1}H NMR spectroscopy.

4.15. Kinetic study of asymmetric hydroamination/cyclization

In a typical experiment, a screw cap NMR tube was charged in the glovebox with the corresponding precatalyst (2–5 mg), C_6D_6 (0.5 mL) and the substrate (20–35 equiv) in that order. The NMR tube was then placed in the thermostated probe of the Bruker Avance 400 spectrometer. The conversion was monitored by ^{1}H NMR spectroscopy by following the disappearance of the olefinic signals of the substrate relative to the signals of the products. NMR spectra were collected in appropriate time intervals (e.g. 5, 10, 15, 30 or 60 min) using the multizg script from the Bruker XWinNMR software package. In order to ensure accurate integration, a long pulse delay (10 s) was used during data acquisition. Kinetic data for the hydroamination reactions were fitted by least-squares methods to Eq. (1), were C_0 is the initial concentration of the substrate and C is the substrate concentration at time t (min).

$$(C_0 - C)/C_0 = a \times t \quad (1)$$

The turnover frequency, N_t (h^{-1}), was calculated from the least-squares determined slope (a) according to Eq. (2).

$$N_t\left(\mathrm{h}^{-1}\right) = -\left(60\ \mathrm{min\ h}^{-1}\right) \times a/[\mathrm{catalyst}]_0 \quad (2)$$

Acknowledgment

Generous financial support by the Deutsche Forschungsgemeinschaft (Emmy Noether Programme) and the National Science Foundation (NSF CAREER Award CHE 0956021) is gratefully acknowledged.

Appendix A. Supplementary material

CCDC-785394 and CCDC-785395 contains the supplementary crystallographic data for this paper. These data can be obtained free of charge from The Cambridge Crystallographic Data Centre via www.ccdc.cam.ac.uk/data_request/cif.

References

[1] General reviews on hydroamination are provided in: (a) T.E. Müller, K.C. Hultzsch, M. Yus, F. Foubelo, M. Tada, Chem. Rev. 108 (2008) 3795–3892; (b) S. Doye, in: D. Enders (Ed.), Science of Synthesis, vol. 40a, Georg Thieme Verlag, Stuttgart, 2009, pp. 241–304; (c) T.E. Müller, M. Beller, Chem. Rev. 98 (1998) 675–703; (d) J.J. Brunet, D. Neibecker, in: A. Togni, H. Grützmacher (Eds.), Catalytic Heterofunctionalization from Hydroamination to Hydrozirconation, Wiley-VCH, Weinheim, 2001, pp. 91–141.

[2] For selected reviews on more specialized aspects of hydroamination see: (a) J. Seayad, A. Tillack, C.G. Hartung, M. Beller, Adv. Synth. Catal 344 (2002) 795–813; (b) M. Beller, C. Breindl, M. Eichberger, C.G. Hartung, J. Seayad, O.R. Thiel, A. Tillack, H. Trauthwein, Synlett (2002) 1579–1594; (c) F. Pohlki, S. Doye, Chem. Soc. Rev. 32 (2003) 104–114; (d) I. Bytschkov, S. Doye, Eur. J. Org. Chem. (2003) 935–946; (e) S. Doye, Synlett (2004) 1653–1672; (f) S. Hong, T.J. Marks, Acc. Chem. Res. 37 (2004) 673–686; (g) J.F. Hartwig, Pure Appl. Chem. 76 (2004) 507–516; (h) A.L. Odom, Dalton Trans. (2005) 225–233; (i) R.A. Widenhoefer, X. Han, Eur. J. Org. Chem. (2006) 4555–4563; (j) R. Severin, S. Doye, Chem. Soc. Rev. 36 (2007) 1407–1420; (k) J.-J. Brunet, N.-C. Chu, M. Rodriguez-Zubiri, Eur. J. Inorg. Chem. (2007) 4711–4722; (l) T. Andrea, M.S. Eisen, Chem. Soc. Rev. 37 (2008) 550–567; (m) J.G. Taylor, L.A. Adrio, K.K. Hii, Dalton Trans. 39 (2010) 1171–1175.

[3] (a) M.R. Crimmin, M. Arrowsmith, A.G.M. Barrett, I.J. Casely, M.S. Hill, P.A. Procopiou, J. Am. Chem. Soc. 131 (2009) 9670–9686; (b) S. Datta, M.T. Gamer, P.W. Roesky, Organometallics 27 (2008) 1207–1213; (c) C. Quinet, P. Jourdain, C. Hermans, A. Ates, I. Lucas, I.E. Marko, Tetrahedron 64 (2008) 1077–1087; (d) T. Ogata, A. Ujihara, S. Tsuchida, T. Shimizu, A. Kaneshige, K. Tomioka, Tetrahedron Lett. 48 (2007) 6648–6650; (e) P. Horrillo-Martínez, K.C. Hultzsch, A. Gil, V. Branchadell, Eur. J. Org. Chem. (2007) 3311–3325; (f) P. Horrillo Martínez, K.C. Hultzsch, F. Hampel, Chem. Commun. (2006) 2221–2223; (g) P. Horrillo-Martínez, K.C. Hultzsch, Tetrahedron Lett. 50 (2009) 2054–2056.

[4] For a more general review of the application of organo rare-earth metal catalysts in organic synthesis see: (a) A.L. Reznichenko, K.C. Hultzsch, Struct. Bond. 137 (2010) 1–48; (b) G.A. Molander, J.A.C. Romero, Chem. Rev. 102 (2002) 2161–2185; (c) G.A. Molander, E.C. Dowdy, Top. Organomet. Chem. 2 (1999) 119–154.

[5] (a) M.R. Gagné, C.L. Stern, T.J. Marks, J. Am. Chem. Soc. 114 (1992) 275–294; (b) M.A. Giardello, V.P. Conticello, L. Brard, M.R. Gagné, T.J. Marks, J. Am. Chem. Soc. 116 (1994) 10241–10254; (c) J.-S. Ryu, T.J. Marks, F.E. McDonald, J. Org. Chem. 69 (2004) 1038–1052; (d) S. Hong, A.M. Kawaoka, T.J. Marks, J. Am. Chem. Soc. 125 (2003) 15878–15892; (e) M.R. Douglass, M. Ogasawara, S. Hong, M.V. Metz, T.J. Marks, Organometallics 21 (2002) 283–292.

[6] For reviews on asymmetric hydroamination see: (a) P.W. Roesky, T.E. Müller, Angew. Chem. Int. Ed. 42 (2003) 2708–2710; (b) K.C. Hultzsch, Adv. Synth. Catal. 347 (2005) 367–391; (c) K.C. Hultzsch, Org. Biomol. Chem. 3 (2005) 1819–1824; (d) K.C. Hultzsch, D.V. Gribkov, F. Hampel, J. Organomet. Chem. 690 (2005) 4441–4452; (e) I. Aillaud, J. Collin, J. Hannedouche, E. Schulz, Dalton Trans. (2007) 5105–5118; (f) G. Zi, Dalton Trans. (2009) 9101–9109; (g) S.R. Chemler, Org. Biomol. Chem. 7 (2009) 3009–3019; (h) A.L. Reznichenko, K.C. Hultzsch, in: T. Nugent (Ed.), Chiral Amine Synthesis: Methods, Developments and Applications, Wiley-VCH, Weinheim, 2010, pp. 341–375.

[7] (a) P.N. O'Shaughnessy, P.D. Knight, C. Morton, K.M. Gillespie, P. Scott, Chem. Commun. (2003) 1770–1771;
(b) P.N. O'Shaughnessy, P. Scott, Tetrahedron: Asymmetry 14 (2003) 1979–1983;
(c) S. Hong, S. Tian, M.V. Metz, T.J. Marks, J. Am. Chem. Soc. 125 (2003) 14768–14783;
(d) J.Y. Kim, T. Livinghouse, Org. Lett. 7 (2005) 1737–1739;
(e) D. Riegert, J. Collin, A. Meddour, E. Schulz, A. Trifonov, J. Org. Chem. 71 (2006) 2514–2517;
(f) N. Meyer, A. Zulys, P.W. Roesky, Organometallics 25 (2006) 4179–4182;
(g) X. Yu, T.J. Marks, Organometallics 26 (2007) 365–376;
(h) I. Aillaud, J. Collin, C. Duhayon, R. Guillot, D. Lyubov, E. Schulz, A. Trifonov, Chem. Eur. J. 14 (2008) 2189–2200;
(i) G. Zi, L. Xiang, H. Song, Organometallics 27 (2008) 1242–1246;
(j) I. Aillaud, D. Lyubov, J. Collin, R. Guillot, J. Hannedouche, E. Schulz, A. Trifonov, Organometallics 27 (2008) 5929–5936.
[8] (a) D.V. Gribkov, K.C. Hultzsch, F. Hampel, Chem. Eur. J. 9 (2003) 4796–4810;
(b) D.V. Gribkov, F. Hampel, K.C. Hultzsch, Eur. J. Inorg. Chem. (2004) 4091–4101;
(c) D.V. Gribkov, K.C. Hultzsch, Chem. Commun. (2004) 730–731;
(d) D.V. Gribkov, K.C. Hultzsch, F. Hampel, J. Am. Chem. Soc. 128 (2006) 3748–3759;
(e) D.V. Vitanova, F. Hampel, K.C. Hultzsch, J. Organomet. Chem. 692 (2007) 4690–4701;
(f) A.L. Reznichenko, F. Hampel, K.C. Hultzsch, Chem. Eur. J. 15 (2009) 12819–12827;
(g) A.L. Reznichenko, H.N. Nguyen, K.C. Hultzsch, Angew. Chem. Int. Ed. 49 (2010) doi:10.1002/anie.201004570.
[9] Chiral catalyst systems for the hydroamination/cyclization of aminoalkenes based on metals other than rare-earth metals: (a) D.A. Watson, M. Chiu, R.G. Bergman, Organometallics 25 (2006) 4731–4733;
(b) M.C. Wood, D.C. Leitch, C.S. Yeung, J.A. Kozak, L.L. Schafer, Angew. Chem. Int. Ed. 46 (2007) 354–358;
(c) A.L. Gott, A.J. Clarke, G.J. Clarkson, P. Scott, Organometallics 26 (2007) 1729–1737;
(d) G. Zi, F. Zhang, L. Xiang, Y. Chen, W. Fang, H. Song, Dalton Trans. 39 (2010) 4048–4061;
(e) X. Shen, S.L. Buchwald, Angew. Chem. Int. Ed. 49 (2010) 564–567.
[10] (a) D.V. Vitanova, F. Hampel, K.C. Hultzsch, Dalton Trans. (2005) 1565–1566;
(b) D.V. Vitanova, F. Hampel, K.C. Hultzsch, J. Organomet. Chem. 690 (2005) 5182–5197.
[11] For related linked aminotroponiminate complexes of the rare-earth metals see ref. 7f as well as: (a) P.W. Roesky, Inorg. Chem. 37 (1998) 4507;
(b) P.W. Roesky, M.R. Bürgstein, Inorg. Chem. 38 (1999) 5629;
(c) M.R. Bürgstein, P.W. Roesky, Organometallics 22 (2003) 1372.
[12] For a general review of the chemistry of β-diketiminato ligands see: L. Bourget-Merle, M.F. Lappert, J.R. Severn Chem. Rev. 102 (2002) 3031–3065.
[13] S. Gong, H. Ma, J. Huang, Dalton Trans. (2009) 8237–8247.
[14] For additional studies on linked bis(β-diketiminato) complexes see: (a) L. Bourget-Merle, P.B. Hitchcock, M.F. Lappert, J. Organomet. Chem. 689 (2004) 4357–4365;
(b) B.Y. Lee, H.Y. Kwon, S.Y. Lee, S.J. Na, S.-I. Han, H. Yun, H. Lee, Y.-W. Park, J. Am. Chem. Soc. 127 (2005) 3031–3037;
(c) M.F. Pilz, C. Limberg, B. Ziemer, J. Org. Chem. 71 (2006) 4559–4564;
(d) T.J. Hebden, W.W. Brennessel, C.J. Flaschenriem, P.L. Holland, Dalton Trans. (2006) 3855–3857;
(e) M.F. Pilz, C. Limberg, B.B. Lazarov, K.C. Hultzsch, B. Ziemer, Organometallics 26 (2007) 3668–3676;
(f) J. Vela, L. Zhu, C.J. Flaschenriem, W.W. Brennessel, R.J. Lachicotte, P.L. Holland, Organometallics 26 (2007) 3416–3423;
(g) M.F. Pilz, C. Limberg, S. Demeshko, F. Meyer, B. Ziemer, Dalton Trans. (2008) 1917–1923;
(h) D.F.-J. Piesik, S. Range, S. Harder, Organometallics 27 (2008) 6178–6187;
(i) D.F.-J. Piesik, P. Haack, S. Harder, C. Limberg, Inorg. Chem. 48 (2009) 11259–11264.
[15] K.C. Hultzsch, F. Hampel, T. Wagner, Organometallics 23 (2004) 2601–2612.
[16] (a) J. Eppinger, M. Spiegler, W. Hieringer, W.A. Herrmann, R. Anwander, J. Am. Chem. Soc. 122 (2000) 3080–3096;
(b) R.R. Fraser, S.T. Mansour, S. Savard, J. Org. Chem. 50 (1985) 3232–3234.
[17] M.E. Jung, G. Piizzi, Chem. Rev. 105 (2005) 1735–1766.
[18] (a) D.C. Bradley, J.S. Ghotra, F.A. Hart, J. Chem. Soc., Dalton Trans. (1973) 1021–1023;
(b) Y. Mu, W.E. Piers, M.-A. MacDonald, M.J. Zaworotko, Can. J. Chem. 73 (1995) 2233–2238.
[19] Y. Tamaru, M. Hojo, H. Higashimura, Z.-I. Yoshida, J. Am. Chem. Soc. 110 (1988) 3994–4002.
[20] C.F. Bender, R.A. Widenhoefer, J. Am. Chem. Soc. 127 (2005) 1070–1071.
[21] (a) F. Galsbol, P. Steenbol, B.S. Sorensen, Acta. Chem. Scand 26 (1972) 3605–3611;
(b) J.F. Larrow, E.N. Jacobsen, Y. Gao, Y. Hong, X. Nie, C.M. Zepp, J. Org. Chem. 59 (1994) 1939–1942.
[22] P.M. Smith, E.J. Thomas, J. Chem, Soc. Perkin Trans. 1 (1998) 3541–3556.
[23] (a) "Collect" Data Collection Software. Nonius B. V, 1998;
(b) Z. Otwinowski, W. Minor, "Scalepack" Data Processing Software, , In: Methods in: Enzymology (Macromolecular Crystallography, Part A), vol. 276 (1997) 307;
(c) G.M. Sheldrick, SHELX-97, program for the refinement of crystal structures. University of Göttingen, 1997;
(d) D.T. Cromer, J.T. Waber, in: J.A. Ibers, W.C. Hamilton (Eds.), International Tables for X-ray Crystallography, Kynoch, Birmingham, Great Britain, 1974.